Original Article

www.anatomy.org.tr

Received: June 15, 2009; Accepted: August 13, 2009; Published online: August 24, 2009

doi:10.2399/ana.09.019

anatomy
International Journal of Experimental and Clinical Anatomy

Three-dimensional reconstruction and volume calculation of the intraorbital part of the optic nerve with high resolution MRI

İlkan Tatar[1], Işıl Saatçi[2], Meserret Cumhur[1]

[1]*Department of Anatomy, Medical School, Hacettepe University, Ankara, Turkey*

[2]*Department of Radiology, Medical School, Hacettepe University, Ankara, Turkey*

Abstract

Objectives: Rapid improvements on MRI techniques in recent years brought the investigation of the optic nerve involvement in demyelinating diseases in a detailed manner. This revealed the need to establish standard criteria on defining the pathological conditions related to geriatric population such as optical atrophy, which is more frequently seen in developed countries as well as in our country. This than directed neuroanatomical and neuroradiological studies to the structures like optic nerve that is smaller and hence more difficult to identify with routine MRI sequences. Our aim was to obtain 3D reconstruction and volume calculation of the intraorbital part of the optic nerve from sequential MRI sections.

Methods: In this study, 24 female and 24 male volunteers, aged between 20 and 40 have been investigated with T2 weighted MRI sequences with 2mm intervals. The imaging procedures have been performed with Siemens Allegra MRI equipment which has 3 Tesla of magnetic power. Approximately 10 serial sections, from the bulbus oculi to the optic canal, have been used to get the three-dimensional (3D) reconstruction. The 3D reconstruction was produced with the SurfDriver software. The volumes of the intraorbital parts of the optic nerve and their dural sheaths were calculated for either side.

Results: The results have been compared with respect to some variables like age, gender, body mass index (BMI) and blood pressure. There was not any statistically significant difference between the volumes with respect to age, gender and BMI.

Conclusion: The optic nerve sheath volumes, consequently the subarachnoidal space volumes were significantly increased in either side within the group that had higher values than the normal blood pressure, compared with the normal blood pressure group.

Key words: 3T MRI; intraorbital part of the optic nerve; 3D reconstruction; volume analysis; SurfDriver and Osirix

Anatomy 2009; 3: 49-57, © 2009 TSACA

Introduction

Optic nerve (ON) always takes attractions of the neuroscientists since the period of ancient scientists like Rufus of the Ephesus and Herophilus of the Chalcedon, accepted as the father of the modern Anatomy. Herophilus wrote his discoveries about the eye from his vivo-sections in the treatise called "On the eye".[1] He was first to differentiate between cranial and spinal nerves. He described at least seven pairs of cranial nerves and named six of the pairs as follows: optic, occulomotor, trigeminal, facial, auditory, and hypoglossal. He meticulously differentiated and described at least four coats or membranes of the eye. He named them the cornea, retina, choroid, and iris. He delineated for the first time the ciliary body, which is the thickened portion of the tunica vasculosa between the choroid and the iris. He also described the vitreous humor.[2] When we looked at the

anatomical point of view, the ON was always important and different from other cranial nerves as an elongation of the brain with the olfactory nerve. Again the great scientist from fertile crescent, also called mesopotamia, Ibn al Haytham, al-Basri or Alhazeni in western literature, gave his seven volume marvelous treatise about optics, light and vision theory called "Kitab el-Manazir".[3]

Recently increasing interest on neurosciences, huge research budget for demyelinating diseases like multiple sclerosis (MS) and both qualitative and quantitative developments of imaging modalities especially on MRI are facilitate to observe ON and its pathologies in detailed manner.

ON has a special potential for understanding pathophysiology and to make differential diagnosis of demyelinating diseases especially MS.[4] In addition to this ON diseases like optic neuritis provide very good model for studies on demyelinating diseases to understand pathogenetic mechanisms and to improve trustworthy imaging technique for ON atrophy measurement which facilitates that studies.[5-7]

In that condition MRI comes forward like in all other neurological tissues. At the same time it has several limitations like small size and tortuous course of ON, high signal conduction due to periorbital fat tissue and coverings fulfilled with cerebro-spinal fluid (CSF) and motion artifacts due to close bony neighborhood and possible eye movements. But all these limitations can be surpassed by the options of developments on MRI technology and it is possible to understand anatomical and physiological imaging characteristics of ON and its surroundings both in normal and pathological conditions.

Hickman et al.[5] and Votruba et al.[8] made area calculations for ON and its surrounding dural sheath in the MRI studies of optic neuritis and optic atrophy respectively. In this study we aimed that three-dimensional (3D) reconstruction and volume calculation of the intraorbital part of the ON from serial sequential coronal sections of high resolution (3 Tesla) MRI for better understanding of normal course and anatomy of the ON and to associate it with pathophysiologies of the demyelinating diseases.

Materials and Methods

In this study we used digital imaging and communication on medicine (DICOM)[9] images acquired from 3T Siemens Allegra MRI scanner at Hacettepe University Hospital, Department of Radiology MRI center. Because it was a definitive study with reconstructive modeling technique and volume calculation, the sample pool consisted of 24 male and 24 female volunteers who had no known or MRI visible brain pathology and between 20 and 40 years old, equally distributed in 21 to 30 and 31 to 40 age periods. Weight, height, diastolic and systolic arterial pressure of each subject was recorded at imaging center.

Routine brain MRI protocol of Hacettepe University Hospital, Department of Radiology MRI center was applied all volunteers and than, after the approval of experienced neuroradiologist as a normal, additional 11 minute T2 weighted turbo spin echo (TSE), fat saturated (FATSAT) sequence with time to relaxation (TR) 4970 ms, time to echo (TE) 101 ms, 2 mm section thickness and 30 sequential coronal oblique sections **(Figure 1)** was performed to finish imaging procedure.

From the 30 sequential coronal oblique sections, intraorbital part of the ON was determined by an experienced neuroradiologist and anatomist in DICOM viewer software (OsiriX[10,11] by Antoine Rosset) as anteri-

Figure 1. T2 weighted FATSAT coronal oblique image seen on the user interface of Osirix. Three dimensional reconstruction and volume calculation is to be performed.

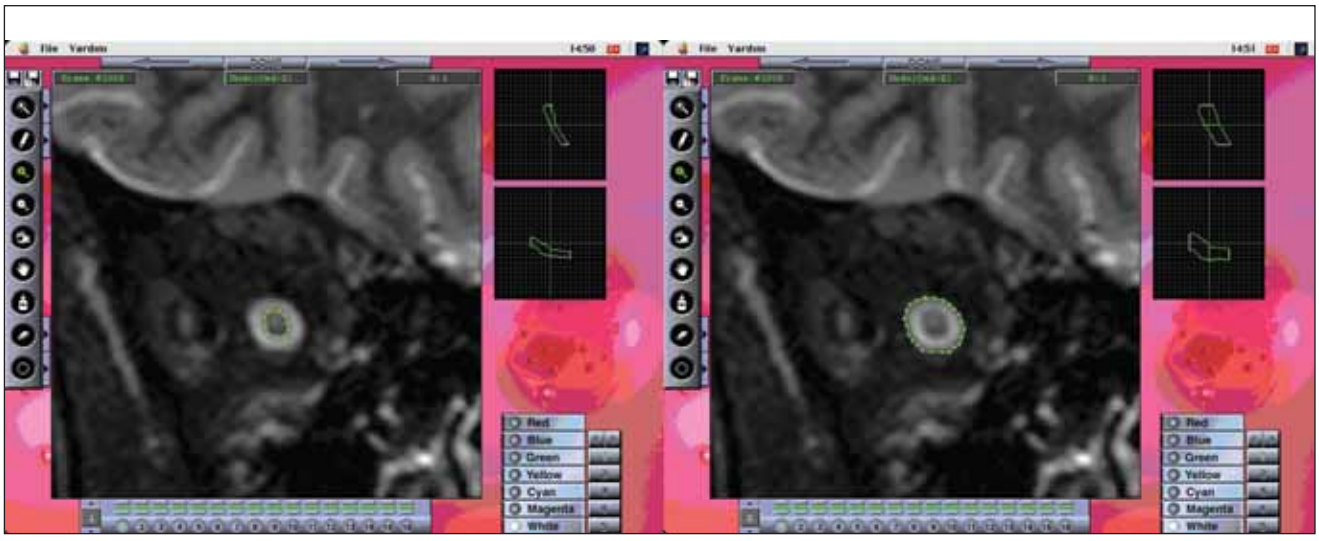

Figure 2. Manually contoured ON and its dural sheath on the user interface of Surf Driver.

or border was just behind the eye ball and posterior border was the entry of the optic canal. After that DICOM images were converted into.jpg file format which was the main file format for reconstruction software (Surf Driver 3.5.312 by David Moody and Scott Lozanoff). In the interface of Surf Driver software, left and right ON and their hyper intense subarachnoidal spaces and dural sheaths were meticulously contoured by an anatomist to create a 3D model **(Figures 2** and **3).** Volume calculations of these models were made by volume analysis tool in the interface of the software **(Figure 4).**

Statistical analysis of the study was made by using SPSS 10.0 software. Volume calculations of the models were statistically compared with Continuity Correction and Fisher's Exact Tests in according to gender, age, body mass index (BMI), diastolic and systolic arterial pressure.

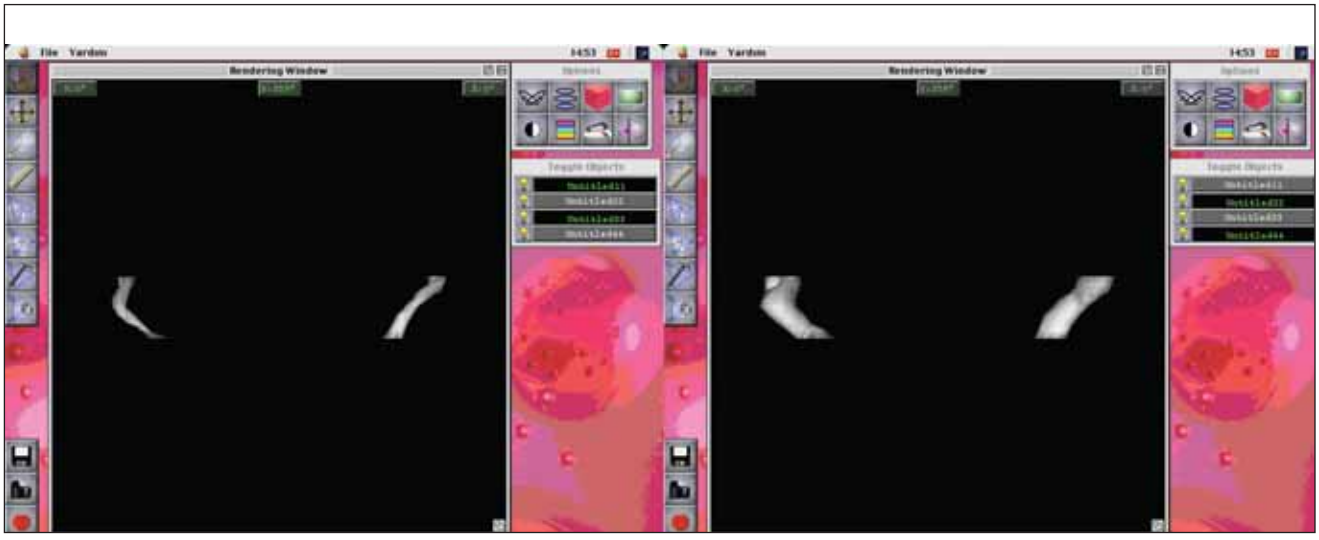

Figure 3. Three dimensional reconstruction models of the left and right ONs and dural sheaths on the user interface of SurfDriver after contouring.

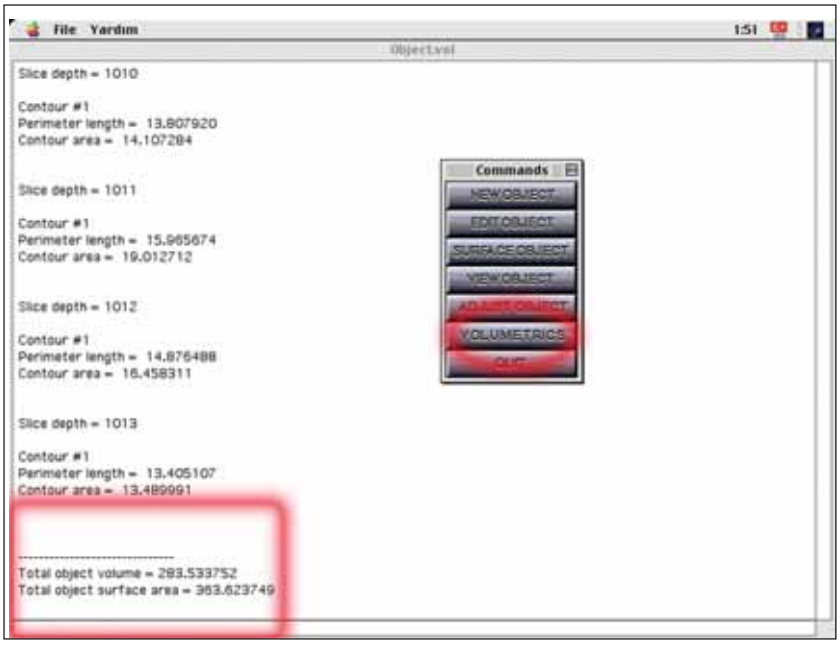

Figure 4. Volume values of the reconstructed models on the user interface of SurfDriver.

Results

Volume calculation results of all samples are shown in **Table 1.**

Sample pool was divided into two groups as Group 1 between 21 to 30 years old and Group 2 between 31 to 40 years old. The volume values of these groups are seen in **Table 2.** There was no statistically significant difference between the two groups with respect to the mean volume value.

Volume disturbance with respect to gender is seen in **Table 3.** After statistical analysis, there was a statistically significant difference between male- and female-only groups in the volume of the left optic nerve which had higher values in males (p=0.01).

Sample pool was divided into two groups with respect to BMI as Group 1 who had BMI less than or equal to 25 and Group 2 who had BMI larger than 26. The volume values of these groups are seen in **Table 4.** There was no statistically significant difference between two groups with respect to the mean volume value.

Volume disturbance with respect to systolic arterial blood pressure (SABP) is seen in **Table 5.** Sample pool was divided into two groups with respect to SABP as Group 1 who had normal SABP less than or equal to 120 mmHg and Group 2 who had increased SABP larger than 121 mmHg. After statistical analysis, there was a statistically significant difference between normal and increased SABP in the volumes of the right and left dural sheaths which had higher values in the increased SABP

Table 1
Volume values of optik nerve and its dural sheaths

Volumes (mm^3)	Total	Minimum	Maximum	Mean	SD
Right ON volume	48	181.9	329.1	247.3	36.9
Right dural sheath volume	48	689.0	1279.0	948.5	134.7
Left ON volume	48	165.7	321.9	234.8	43.3
Left dural sheath volume	48	684.4	1316.3	942.8	151.8

ON: optic nerve; **SD:** standart deviation

Table 2
Distribution of the volume values with respect to age

Volumes (mm^3)	Group	Number	Mean	SD	SEM
Right ON volume	1	24	250.7	28.2	5.8
Right ON volume	2	24	244.0	44.4	9.1
Right dural sheath volume	1	24	946.3	113.7	23.2
Right dural sheath volume	2	24	950.7	155.3	31.7
Left ON volume	1	24	232.8	40.5	8.3
Left ON volume	2	24	236.9	46.6	9.5
Left dural sheath volume	1	24	929.8	144.2	29.4
Left dural sheath volume	2	24	955.7	161.1	32.9

ON: optic nerve; **SD:** standart deviation; **SEM:** standard error of the mean

Table 3
Distribution of the volume values with respect to gender

Volumes (mm^3)	Gender	Number	Mean value	SD	SEM
Right ON volume	1	24	257.533	26.5062	5.4106
Right ON volume	2	24	237.121	43.1930	8.8167
Right dural sheath volume	1	24	962.570	107.1340	21.869
Right dural sheath volume	2	24	934.380	158.643	32.383
Left ON volume	1	24	250.704	29.8636	6.0959
Left ON volume	2	24	218.987	49.0679	10.0159
Left dural sheath volume	1	24	960.712	105.2292	21.4798
Left dural sheath volume	2	24	924.813	188.0549	38.3865

ON: optic nerve; **SD:** standart deviation; **SEM:** standard error of the mean

group (p=0.03 for the right and p=0.02 for the left dural sheath).

Volume disturbance with respect to diastolic arterial blood pressure (DABP) is seen in **Table 6.** Sample pool was divided into two groups with respect to DABP as Group 1 who had normal DABP < and equal 80 mmHg and Group 2 who had increased DABP > 81 mmHg. After statistical analysis, there was a statistically significant difference between normal and increased DABP in the volumes of the right and left dural sheaths which had higher values in the increased DABP group (p=0.01 for the right and p=0.02 for the left dural sheath).

Table 4
Distribution of the volume values with respect to body mass index (BMI)

Volumes (mm^3)	BMI	Number	Mean	SD	SEM
Right ON volume	1	38	242.326	38.2934	6.212
Right ON volume	2	10	266.33	24.1553	7.6386
Right dural sheath volume	1	38	930.53	130.587	21.184
Right dural sheath volume	2	10	1016.68	134.438	42.513
Left ON volume	1	38	230.092	45.4205	7.3682
Left ON volume	2	10	252.91	28.8793	9.1325
Left dural sheath volume	1	38	926.861	156.9996	25.4687
Left dural sheath volume	2	10	1003.19	118.041	37.3279

ON: optic nerve; **SD:** standart deviation; **SEM:** standard error of the mean

Table 5
Distribution of the volume values with respect to systolic arterial blood pressure (SABP)

Volumes (mm^3)	SABP	Number	Mean	SD	SEM
Right ON volume	1	46	244.119	37.6385	5.8077
Right ON volume	2	2	269.783	22.4861	9.1799
Right dural sheath volume	1	46	932.86	126.868	19.576
Right dural sheath volume	2	2	1057.78	148.684	60.7
Left ON volume	1	46	230.545	43.2019	6.6662
Left ON volume	2	2	264.950	32.3193	13.1943
Left dural sheath volume	1	46	924.138	148.3507	22.8910
Left dural sheath volume	2	2	1073.13	113.7209	46.4264

ON: optic nerve; **SD:** standart deviation; **SEM:** standard error of the mean

Table 6
Distribution of the volume values with respect to diastolic arterial blood pressure (DABP)

Volumes (mm^3)	DABP	Number	Mean	SD	SEM
Right ON volume	1	43	244.735	37.3549	5.6966
Right ON volume	2	5	269.62	25.9268	11.5948
Right dural sheath volume	1	43	930.56	123.874	18.891
Right dural sheath volume	2	5	1102.54	137.319	61.411
Left ON volume	1	43	232.493	43.2228	6.5914
Left ON volume	2	5	255.08	42.4551	18.9865
Left dural sheath volume	1	43	924.805	146.7384	22.3774
Left dural sheath volume	2	5	1097.2	107.3121	47.9914

ON: optic nerve; **SD:** standart deviation; **SEM:** standard error of the mean

Discussion

Before discussing MRI investigation of the ON, we should indicate one CT study with a large sample size. Liu et al. calculated many parameters including longitudinal and transverse diameter of the entry and exit of the optic canal in axial and coronal CT sections of 200 adults.[13] They found average transverse diameter of the canal was 3.57±0.61 mm and longitudinal one was 4.82±0.38 mm and these results agree with our data.

For quantitative MRI of the ON; high field resolution and thin slices must be used. In addition to this, rapid imaging sequences are needed for decreasing the motion artifact. Orbital fatty tissue should be suppressed for visualizing intraorbital part of the nerve. In fact if we have a very bright cerebro-spinal fluid (CSF) signal, we should also try to suppress it. High resolution and thin slices are also needed for decreasing the partial volume effect. Although fat and CSF suppression decrease the contamination effect, they might have some other undesired effects. Motion artifact is a bigger problem in quantitative imaging than it is in qualitative imaging. Thus fast imaging can help in decreasing motion artifact and collecting many different signals in an acceptable time. Above all, signal to noise ratio (SNR), which depends on the slice thickness, pixel dimension and many other parameters, is the most important limiting factor in both qualitative and quantitative imaging.

FATSAT, which increases the visibility of the ON, and short time inversion recovery (STIR) sequences were developed because of the limitations of conventional spin echo (CSE) such as the difficulty to differentiate ON from its surroundings and images being in low resolution acquired in an acceptable scanning time. Both techniques have some disadvantages. STIR sequence needs main magnetic field (B0) homogeneity without

any adverse effects on SNR, FATSAT needs head coil magnetic field (B1) homogeneity with reducing SNR in T1 weighted images. Although typical STIR sequences were used in the previous ON studies, recently FATSAT sequences is preferred with high resolution image quality and increased detection of the lesions.[14] We also used T2 weighted FATSAT images because they facilitate contouring for 3D reconstruction and differentiate ON and surrounding CSF very well. There are also some other sequences, which are used for better visualization of the ON. In a study, which investigated two and three dimensional anatomical comparison of the optic and oculomotor nerves, Held et al.[15] compared three dimensional constructive interference in steady state (3D CISS), 2D TSE T2 weighted and three dimensional magnetization prepared rapid gradient echo (3D MP-RAGE) T1 weighted sequences. They found, especially for the visualization of the ON and its dural sheath, 3D MP-RAGE and 3D CISS had equal sensitivity, 2D TSE had less than other two sequences.

The head coil and FOV size depend on the scanning region for orbital sequences. An 8 cm head coil and 80x40 mm FOV is adequate to visualize the eye balls and orbits of the both sides. It was said that coronal sections with 3 mm thickness were enough for the evaluation of the ON, but we used coronal oblique sections with 2 mm thickness.

Votruba et al. made 3 coronal diameter measurements, first one from the point just behind the eye ball, second one from orbital apex and third one from the point between first two points, for the intraorbital part of the ON in their study about MRI investigation of autosomal dominant (AD) optic atrophy.[8] They found decreased coronal diameters in patients with AD optic athropy compared with the controls. They also realized that the ratio between diameters of the dural sheath and the ON was bigger in study group because of enlargement of subarachnoidal space was relatively bigger than optic atrophy especially at the posterior intraorbital part of the ON. There was a concordance between the measurements applied to the controls in this study and the volume calculation values of our study.

Benign intracranial hypertension, mostly called pseudotumor cerebri, is an increased intracranial pressure condition caused without ventricular obstruction and other causes that cause intracranial pressure increases with normal CSF content. Permanent vision loss is approximately 10% in this disease because of the ON suppression. Gass et al. investigated anomalies of the ON and its CSF filled dural sheath with local coils and fast spin echo (FSE) sequence.[16] They found that the dimension of the subarachnoidal space that covers the ON was not equal in the course of the ON, the widest part was just behind the eye ball, and dural sheath was narrowed to the optic canal in both study and control group.

Sallomi et al. observed opening a small window, 2x3 mm, at the medial side of the dural sheath of the ON as a therapeutic modality of the pseudotumor cerebri.[17] They found that preoperative bilateral enlargements of the subarachnoidal spaces were lost in postoperative period and MRI was the golden standard for the evaluation of the therapy effectiveness with showing fluid collection into the intraorbital tissues and CSF volume decreasing around the ON.

We decided to study on 3D reconstruction and volume calculation of the ON after had realized that Hickman et al. made area measurements on the intraorbital part of the nerve in many different diseases.[5,18-20] In 2001, they used T2 weighted, FATSAT and fluid attenuation inversion recovery (FLAIR) sequence with 5 serial coronal sections, starting from orbital apex and have 3 m section interval, to make field measurements for ON atrophy after single unilateral optic neuritis attack. We used very similar T2 weighted and FATSAT sequence with 10 consequent coronal oblique sections, between eye ball and optic canal and have 2 mm section interval, for 3D reconstruction and volume calculations. Hickman et al.[18] used computer aided contouring method, which was designed by Grimaud et al.[21], in their studies. We used manual contouring software, called SurfDriver that was improved by Scott Lozanoff and David Moody, for this study.

They found mean area of the intraorbital part of the ON at the onset of the unilateral optic neuritis as 16.1 mm^2 and contralateral normal side was 13.4 mm^2. The control group value was 13.6 mm^2. After 1 year follow-up the values were 11.3 mm^2, 12.8 mm^2 and 13.1 mm^2

respectively.[19] They observed that the swelling of the ON shown in the beginning was going to become an atrophy when compared with the contralateral normal eye and both eyes of the control group. They also explained that the recovery of the vision, due to swelling of the nerve and vasogenic edema, that inhibits the conduction of the normal axons, was decreased in first 3 months after optic neuritis attack. After this decrease they hypothesized two reasons which leaded the nerve to the atrophy. First one, originally belonged to Trapp et al.,[22] was the wallerian degeneration of the axons that was injured before in the acute attack and second one was the delayed death of the permanently demyelinating axons like Scolding and Franklin[23] said.

Hickman et al. also investigated frequency of the dural sheath enlargement in acute optic neuritis patients with FATSAT and FSE sequence.[5] They found that the enlargement of the dural sheath was shown more frequently in the anterior part of the nerve but it was not the indicator of the bad prognosis. Additionally contrast agent enhancement of the dural sheath was a typical symptom of the acute optic neuritis and it was not accepted as an inflammatory or infiltrative condition of the sheath.

As we apparently saw in the literature; the ON, its surrounding CSF filled subarachnoidal space and the dural sheath were played very important role in understanding pathophysiology, making diagnosis, planning and screening of the treatment modalities of the demyelinating like MS, inflammatory like optic neuritis, idiopathic like pseudotumor cerebri and atrophic diseases like in normal aging process.

And we all know that MRI is the gold standard imaging modality of the ON with high field resolution and special sequences that facilitate to observe ON in detail. Because of this, our study is the first in the literature with 3T high field resolution, 2 mm coronally oblique section interval and volume calculation of the intraorbital part of the ON. Our feature goal is to make volume calculations of the patients who have ON relating pathology and to compare these results with our normal dataset.

Acknowledgement

This study was printed in Turkish as a finishing thesis of Dr. Tatar's Anatomy Proficiency in Medicine Program of Turkish Ministry of Health. The authors are grateful to Dr. Nail Çadallı for language editing, Prof. Dr. M. Mustafa Aldur and Prof. Dr. H. Hamdi Çelik for their inspiration and encouraging belief in this study.

References

1. Staden H.V. Herophilus of Chalcedon: The art of medicine in early Alexandria. Cambridge, UK: Cambridge University Press; 1989. p. 66-182.
2. Wiltse LL, Pait TG. Herophilus of Alexandria (325-255 B.C.). The father of anatomy. *Spine* 1998; 23: 1904-14.
3. NQ Image. Ibn al-Haytham and eye optics. *Neuroquantology* 2005; 2: 149-50.
4. Filippi M, Miller DH. Magnetic resonance imaging in the differential diagnosis and monitoring of the treatment of multiple sclerosis. *Curr Opin Neurol* 1996; 9: 178-86.
5. Hickman SJ, Miszkiel KA, Plant GT, Miller DH. The optic nerve sheath on MRI in acute optic neuritis. *Neuroradiology* 2005; 47: 51-5.
6. Miller D, Barkhof F, Montalban X, Thompson A, Filippi M. Clinically isolated syndromes suggestive of multiple sclerosis, part I: natural history, pathogenesis, diagnosis, and prognosis. *Lancet Neurol* 2005; 4: 281-8.
7. Miller D, Barkhof F, Montalban X, Thompson A, Filippi M. Clinically isolated syndromes suggestive of multiple sclerosis, part 2: non-conventional MRI, recovery processes, and management. *Lancet Neurol* 2005; 4: 341-8.
8. Votruba M, Leary S, Losseff N, et al. MRI of the intraorbital optic nerve in patients with autosomal dominant optic atrophy. *Neuroradiology* 2000; 42: 180-3.
9. http://medical.nema.org/DICOM
10. http://www.osirix-viewer.com
11. Rosset A, Spadola L, Ratib O. OsiriX: an open-source software for navigating in multidimensional DICOM images. *J Digit Imaging* 2004; 17: 205-16.
12. http://image.nih.gov/software/vis_packages.html#surfdriver
13. Lui X, Zhou C, Zhang G, Lin Y, Li S. CT anatomic measurement of the optic canal and its clinical significance. *Zhonghua Er Bi Yan Hou Ke Za Zhi* 2000; 35: 275-7.
14. Barker GJ. Technical issues for the study of the optic nerve with MRI. *J Neurol Sci* 2000; 172: 13-6.

15. Held P, Nitz W, Seitz J, et al. Comparison of 2D and 3D MRI of the optic and oculomotor nerve anatomy. *Clin Imaging* 2000; 24: 337-43.
16. Gass A, Barker GJ, Riordan-Eva P et al. MRI of the optic nerve in benign intracranial hypertension. *Neuroradiology* 1996; 38: 769-73.
17. Sallomi D, Taylor H, Hibbert J, et al. The MRI appearance of the optic nerve sheath following fenestration for benign intracranial hypertension. *Eur Radiol* 1998; 8: 1193-6.
18. Hickman SJ, Brex PA, Brierley CM, et al. Detection of optic nerve atrophy following a single episode of unilateral optic neuritis by MRI using a fat-saturated short-echo fast FLAIR sequence. *Neuroradiology* 2001; 43: 123-8.
19. Hickman SJ, Toosy AT, Jones SJ, et al. A serial MRI study following optic nerve mean area in acute optic neuritis. *Brain* 2004; 127: 2498-505.
20. Hickman SJ. Optic nerve imaging in multiple sclerosis. *J Neuroimaging* 2007; Suppl 1: 42S-45S.
21. Grimaud J, Lai M, Thorpe J, et al. Quantification of MRI lesion load in multiple sclerosis: a comparison of three computer-assisted techniques. *Magn Reson Imaging* 1996; 14: 494-505.
22. Trapp BD, Peterson J, Ransohoff RM, et al. Axonal transaction in the lesions of multiple sclerosis. *N Eng J Med* 1998; 338: 278-85.
23. Scolding N, Franklin R. Axon loss in multiple sclerosis. *Lancet* 1998; 352: 340-1.

Correspondence to: Ilkan Tatar, MD
Department of Anatomy,
Medical School, Hacettepe University
Sihhiye 06100 Ankara
Phone: +90 312 305 21 14; Fax: +90 312 310 71 69
e-mail: ilkan@hacettepe.edu.tr

Conflict of interest statement: No conflicts declared.